

Polarizability-Enhanced Ionic Transport in Rare-Earth-Free Halide–Sulfide Electrolytes: $\text{Li}_2\text{ZrSCl}_{4-x}\text{Br}_x$

Supporting Information

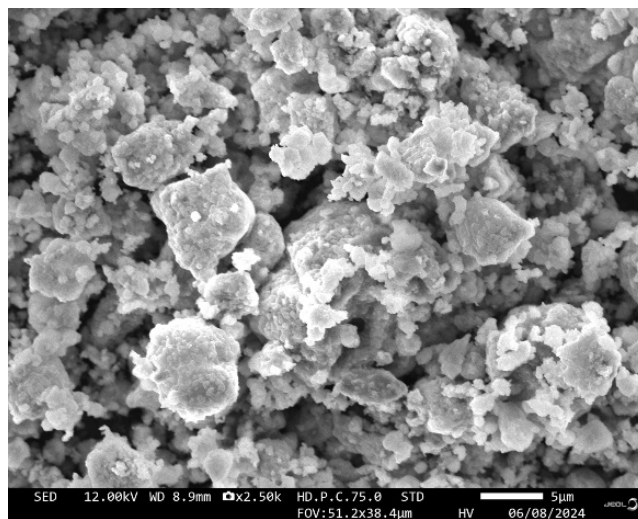


Figure S1: SEM image of $\text{Li}_2\text{ZrSCl}_4$.

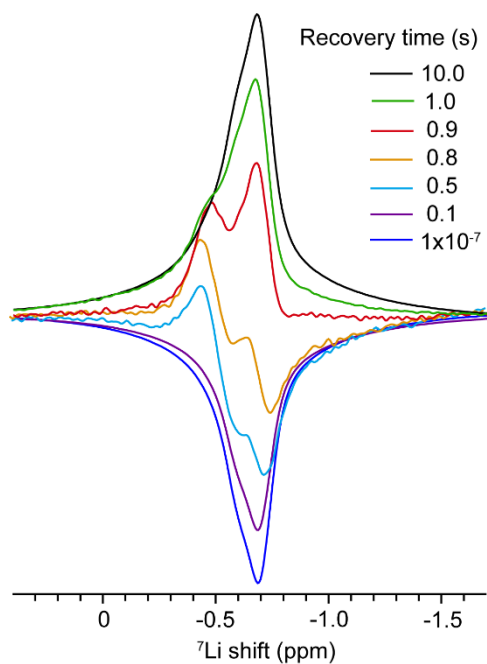


Figure S2: T_1 inversion recovery plots of $\text{Li}_2\text{ZrSCl}_4$ from spin-lattice relaxation experiments collected at various recovery times (τ), after inversion.

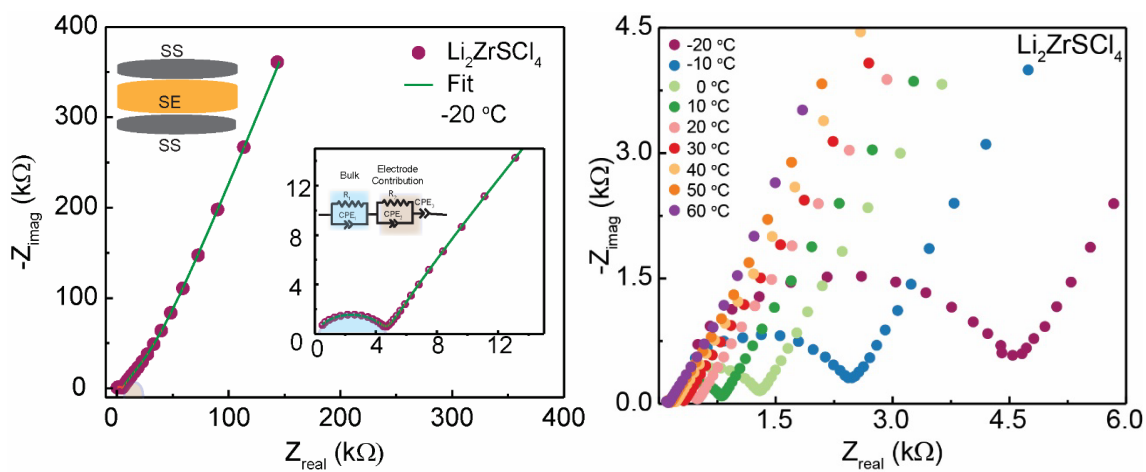


Figure S3: Nyquist plot fitting of LZSC at -20°C (left). Variable-temperature Nyquist plots obtained for $\text{Li}_2\text{ZrSCl}_4$ (right).

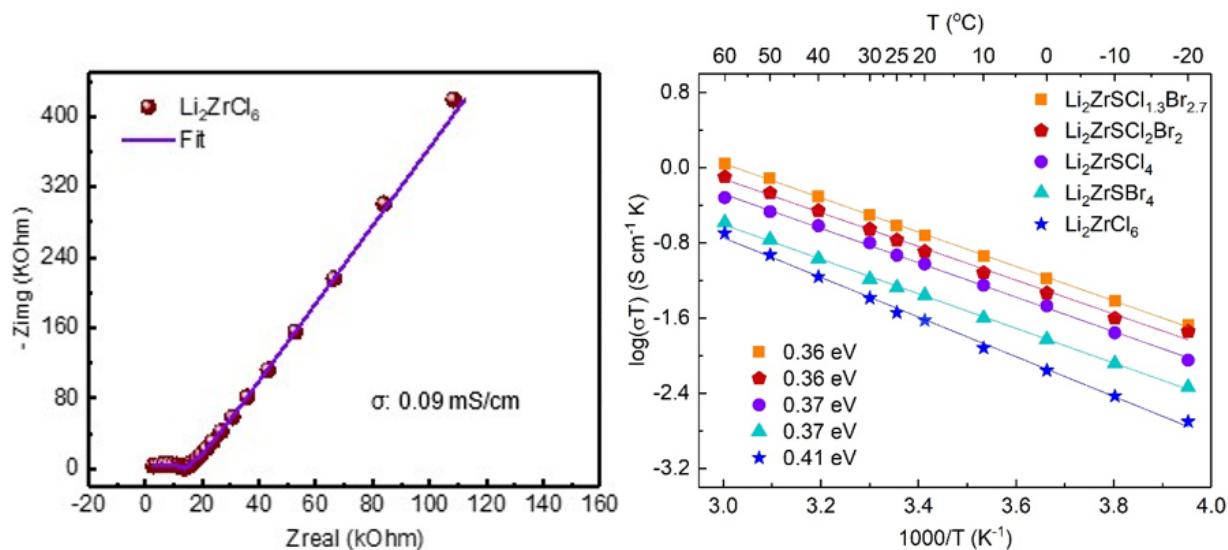


Figure S4: (Left) Fitted Nyquist plot of Li_2ZrCl_6 showing an ionic conductivity of 0.09 mS cm^{-1} . (Right) Combined Arrhenius plot comparing Li_2ZrCl_6 and $\text{Li}_2\text{ZrSCl}_{4-x}\text{Br}_x$ compositions.

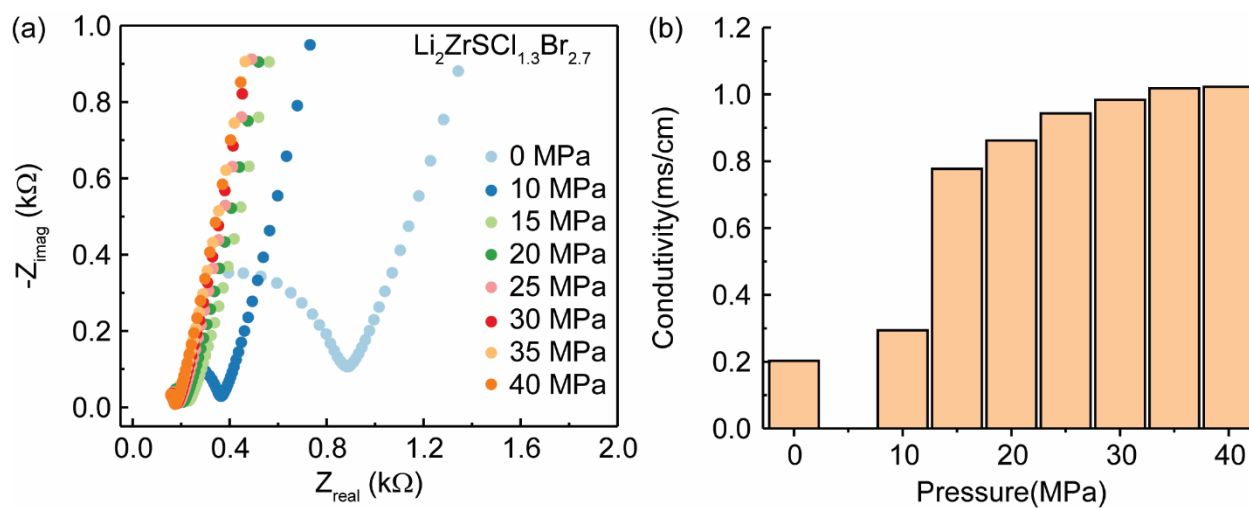


Figure S5. Pressure dependence of the ionic conductivity.

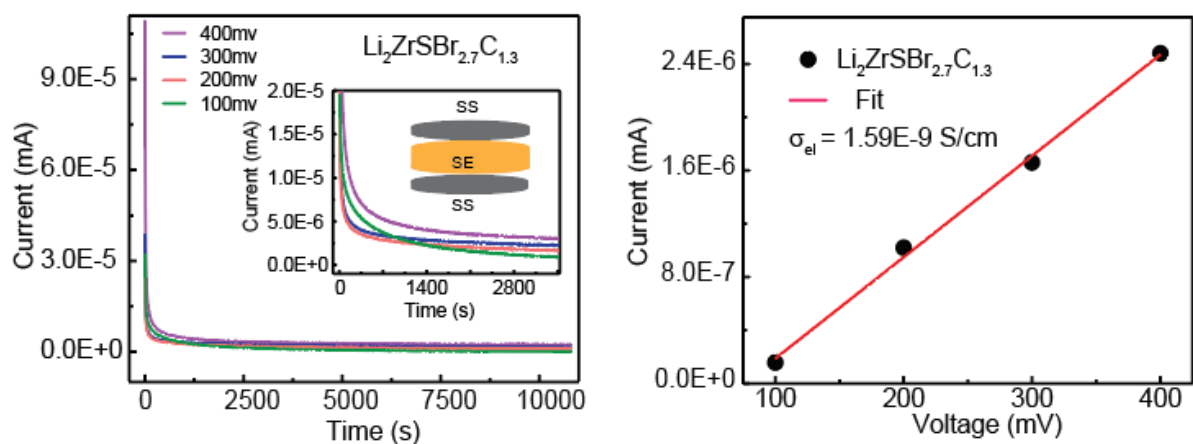


Figure S6: Current vs. time (left) and Current vs. voltage curves (right) of the $\text{Li}_2\text{ZrSBr}_{2.7}\text{C}_{1.3}$ under different DC voltages with the linear fit.

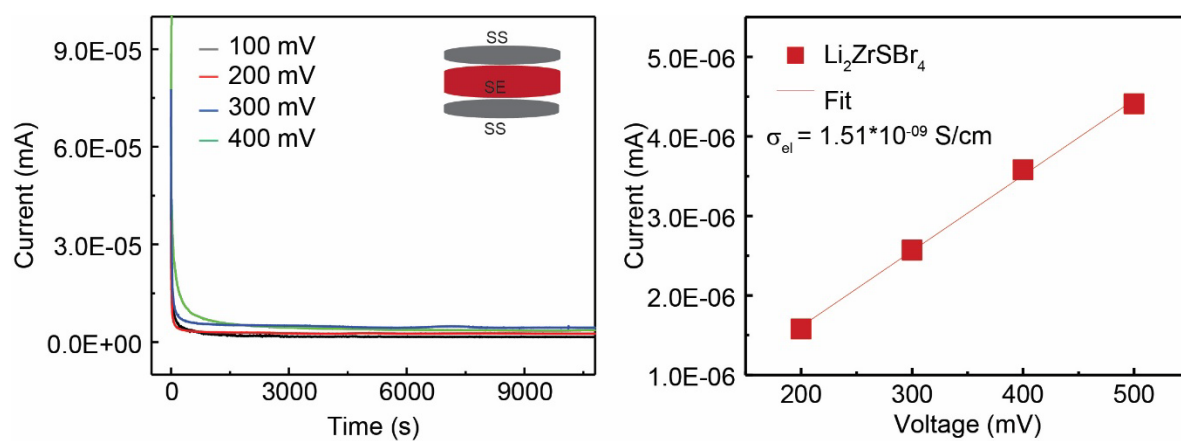


Figure S7: Current vs. time (left) and Current vs. voltage curves (right) of the $\text{Li}_2\text{ZrSBr}_4$ under different DC voltages with the linear fit.

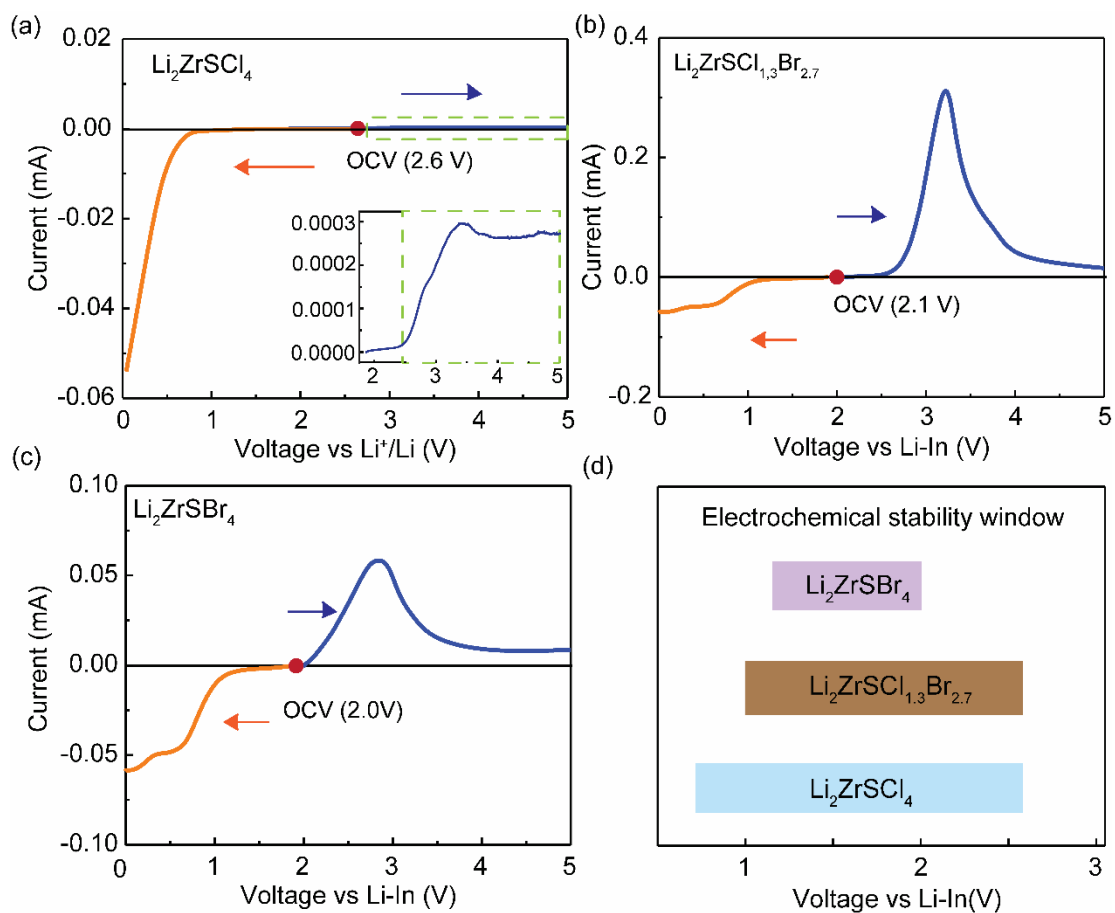


Figure S8: Linear sweep voltammetry curves for evaluating the electrochemical stability window in (a) $\text{Li}_2\text{ZrSCl}_4$, inset is a magnified view of the anodic sweep, (b) $\text{Li}_2\text{ZrSCl}_{1.3}\text{Br}_{2.7}$, (c) $\text{Li}_2\text{ZrSBr}_4$, and (d) the voltage window trend, for comparison.

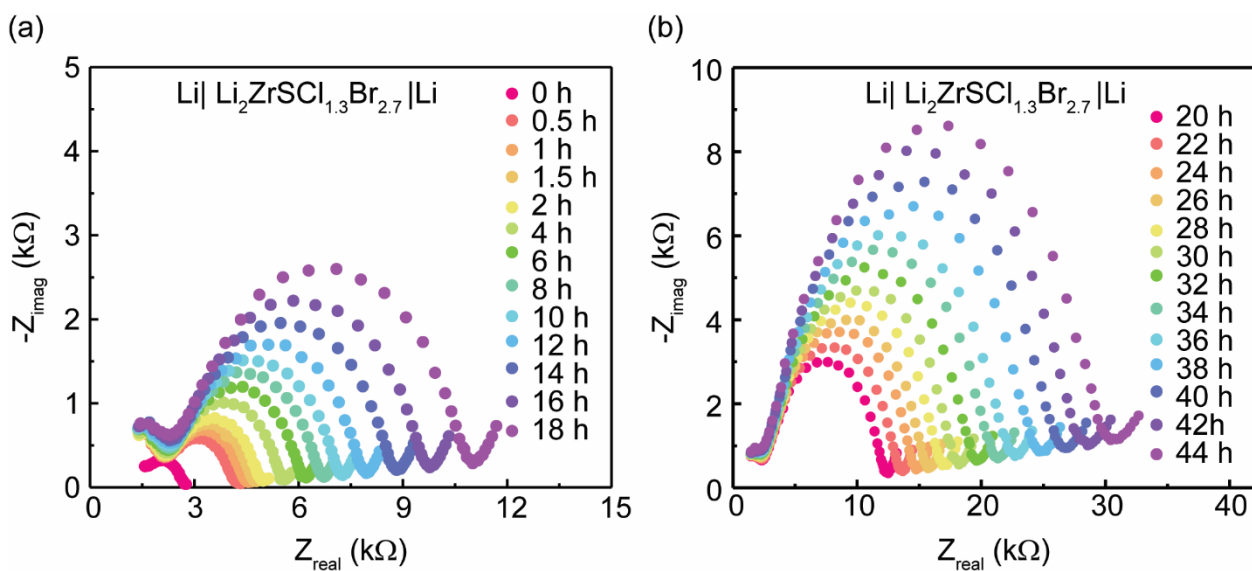


Figure S9. Time-resolved electrochemical impedance spectra of a $\text{Li}|\text{Li}_2\text{ZrSCL}_{1.3}\text{Br}_{2.7}|\text{Li}$ symmetric cell showing progressive impedance growth with increasing polarization time, indicative of continuous interphase formation at the Li-electrolyte interfaces.

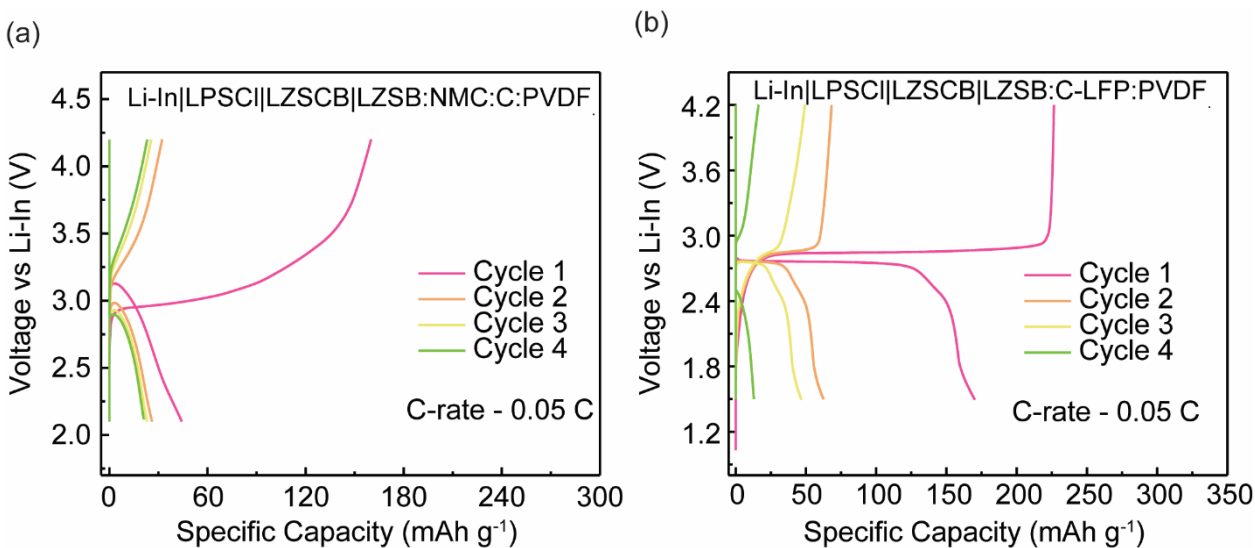


Figure S10: Charge-discharge profiles of all-solid-state cells using $\text{Li}_2\text{ZrSCL}_{1.3}\text{Br}_{2.7}$ as a catholyte with (a) NMC and (b) LFP composite cathodes at 0.05 C, both exhibiting unstable electrochemical behavior and rapid cell failure under the tested conditions.

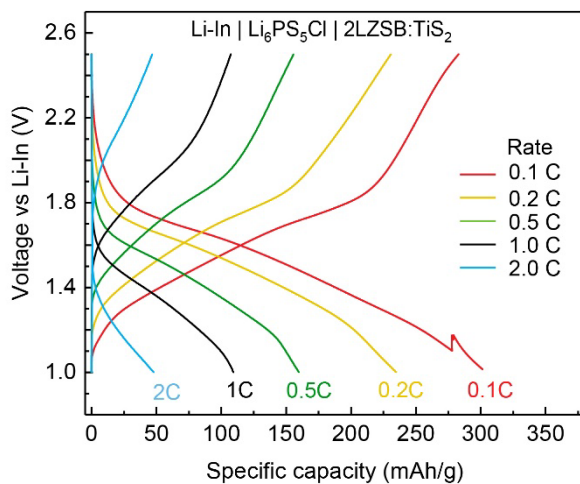


Figure S11: Voltage profile of $\text{Li}_2\text{ZrSBr}_4$

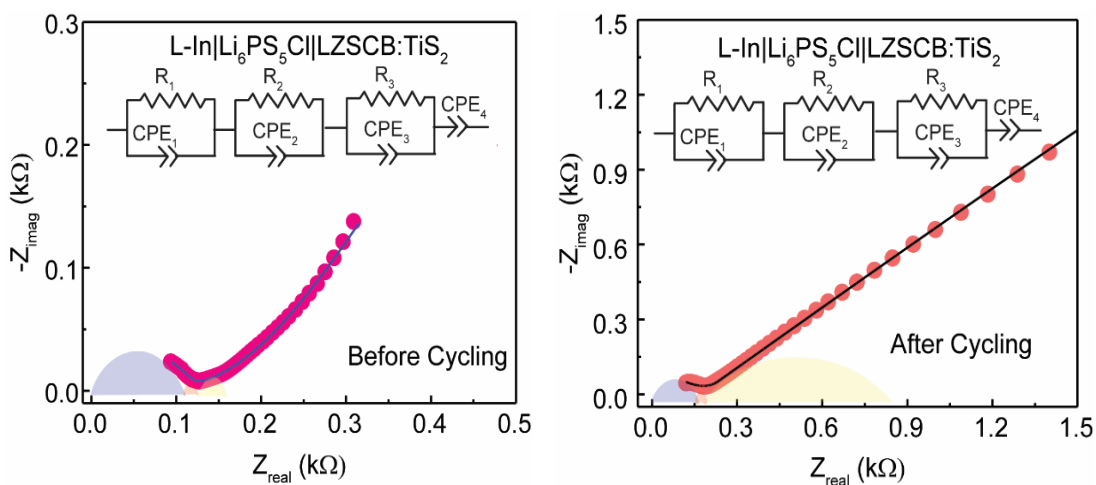


Figure S12: EIS plots with equivalent circuit fitting before and after cycling.

Table S1: Rietveld refinement results from the room-temperature PXRD data of the as-milled $\text{Li}_2\text{ZrSCl}_4$ - $C2/m$ phase.

Lattice parameter: $a = 6.360$, $b = 11.114$, $c = 6.330$, $\alpha = 90.00$, $\beta = 109.73$, $\gamma = 90.00$

Unit-cell volume = 421.17 \AA^3

$R_{\text{wp}} = 4.93 \%$ Crystal system: Hexagonal, Space group: $C2/m$

Name	Atom	Wyckoff position	Atomic coordinates			Occupancy	U_{iso}
			x	y	z		
Li1	Li	4g	0.500	0.816	0.000	0.447	0.310
Li2	Li	4h	0.000	0.148	0.500	0.437	0.010
Li3	Li	2d	0.500	0.000	0.500	0.226	0.429
Zr1	Zr	2a	0.000	0.000	0.000	1.000	0.010
S1	S	4i	0.729	0.000	0.245	0.248	0.006
S2	S	8j	0.238	0.830	0.218	0.126	0.006
Cl1	Cl	4i	0.729	0.000	0.250	0.693	0.006
Cl2	Cl	8j	0.238	0.830	0.218	0.654	0.006

Table S2: Rietveld refinement results from the room-temperature PXRD data of the as-milled $\text{Li}_2\text{ZrSCl}_4$ - $P-3m1$ phase.

Lattice parameter: $a = 11.00$, $b = 11.00$, $c = 5.907$, $\alpha = 90.00$, $\beta = 90.00$, $\gamma = 120.00$

Unit-cell volume = 619.66 \AA^3

$R_{\text{wp}} = 4.93 \%$

Crystal system: Hexagonal, Space group: $P-3m1$

Name	Atom	Wycoff position	Atomic coordinates			Occupancy	U_{iso}
			x	y	z		
Li1	Li	6g	0.311	0.000	0.000	0.412	0.632
Li2	Li	6h	0.322	0.000	0.500	0.595	0.632
Zr1	Zr	1a	0.000	0.000	0.000	0.652	0.025
Zr2	Zr	2d	0.333	0.667	0.548	0.571	0.025
Zr3	Zr	1b	0.000	0.000	0.500	0.712	0.025
Zr4	Zr	2d	0.333	0.667	0.970	0.253	0.025
S1	S	6i	0.106	-0.106	0.760	0.167	0.009
S2	S	6i	0.228	-0.228	0.275	0.167	0.009
S3	S	6i	0.442	-0.442	0.762	0.167	0.009
Cl1	Cl	6i	0.106	-0.106	0.760	0.621	0.009
Cl2	Cl	6i	0.228	-0.228	0.275	0.621	0.009
Cl3	Cl	6i	0.442	-0.442	0.762	0.621	0.009

Table S3: ^6Li NMR Phase Quantification

Chemical Shift	Main Phases (%)		Li ₂ S Phase (%)	Li ₂ S Impurity (wt. %)
	-0.68 ppm	-0.54 ppm	2.4 ppm	
Li ₂ ZrSCl _{1.3} Br _{2.7}	-	83.0	17.0	2.3
Li ₂ ZrSCl ₄	47.7	34.0	18.3	3.6

Table S4: Ionic conductivity and activation energy (E_a) of Li₂ZrSCl_{4-x}Br_x electrolytes.

Sample	Ionic Conductivity (mScm ⁻¹)	Activation Energy (eV)	Prefactor Log σ_0 (KScm ⁻¹)
Li ₂ ZrSCl ₄	0.45	0.37	5.2
Li ₂ ZrSBr ₂ Cl ₂	0.57	0.36	5.3
Li ₂ ZrSBr _{2.7} Cl _{1.3}	1.03	0.36	5.5
Li ₂ ZrSBr ₄	0.43	0.37	4.9

Table S5: Bulk and interfacial resistances from EIS before and after cycling, highlighting interfacial impedance growth during operation.

	Resistant before cycling (Ω)	After cycling (Ω)
R1 - bulk/grain boundary	107.8	146.6
R2 - interface 1	14.87	24.66
R3 - interface 2	35.51	685.5